PUBLICATIONS OF
THE DAVID DUNLAP OBSERVATORY
UNIVERSITY OF TORONTO

VOLUME II NUMBER 7

THE LUMINOSITY FUNCTIONS OF GALACTIC STAR CLUSTERS

SIDNEY VAN DEN BERGH
AND DAVID SHER

1960
TORONTO, CANADA

THE LUMINOSITY FUNCTIONS OF GALACTIC STAR CLUSTERS

Abstract

The luminosity functions of the following galactic clusters have been obtained down to $m_{pg} \simeq 20$

NGC 188	NGC 663	NGC 2158	NGC 2539
NGC 436	NGC 1907	NGC 2194	NGC 2682 (M67)
NGC 457	NGC 1960 (M36)	NGC 2362 (τ CMa)	NGC 7789
NGC 559	NGC 2099 (M37)	NGC 2477	IC 361
NGC 581 (M103)	NGC 2141	NGC 2506	Trumpler 1

It is found that striking differences exist among the main sequence luminosity functions of individual clusters. Also it appears that the faint ends of the luminosity functions of galactic clusters differ systematically from the van Rhijn-Luyten luminosity function for field stars in the vicinity of the sun in the sense that (with one exception) all the clusters which were investigated to faint enough limits, had luminosity functions which either decreased or remained constant below $M_{pg} = +5$. The differences between individual clusters and the differences between the luminosity functions of clusters on the one hand and field stars on the other show that the luminosity function of star creation is not unique. This result is taken to indicate that the luminosity function with which stars are created probably depends on the physical conditions prevailing in the region of star creation.

It is also shown that the observed surface density of cluster stars may be represented by an exponentially decreasing function of the distance from the cluster centre. In a number of clusters, which have ages larger than their relaxation times, the brightest cluster stars are found to be more strongly concentrated towards the cluster centre than are the faintest stars.

Observational Material

This investigation is based on a series of 170 plates of galactic clusters obtained with the 48-inch Schmidt telescope on Palomar Mountain during nine nights in January and February of 1958*. A series of exposures ranging from 4 seconds to 10 minutes on Kodak 103aO emulsion (no filter) was obtained of each cluster. Also one 5-minute exposure of each cluster was taken on Kodak 103aE emulsion behind a red plexiglass filter. The limiting magnitude of each blue plate was determined from a magnitude sequence which had previously been established within the cluster. On each plate stars were counted in rings centred on the cluster. From these counts the number of

*During the night of January 13/14, 1958, the seeing deteriorated rapidly. All plates taken after $19^h\ 15^m$ P.S.T. were subsequently rejected.

cluster stars in each ring down to a given limiting magnitude was determined. By means of this procedure it was possible to investigate the luminosity functions of 20 galactic clusters down to about 20th magnitude.

Counting Procedure

The centre of each cluster was found by inspection and the plate was placed, emulsion downwards, on a sheet of transparent polar graph paper, in such a way that the centre of the cluster coincided with the pole of the co-ordinate system.

The difference in the radii of two consecutive circles of the polar graph paper was 0.1 inches, corresponding to 171″ on the plate. The annuli, henceforth called "rings", thus formed, were numbered 1, 2, 3, etc., from the pole outwards.

Counting stars on a plate is not free from a "personal equation" effect. Innumerable decisions have to be made, rejecting some marks on the plate while accepting others as stars. A comparison between independent counts by the two authors on four plates in M67 is shown in figure 1. The comparison shows that the counts by van den

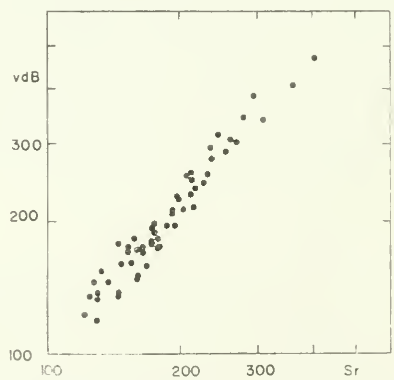

Fig. 1—Comparison of independent counts by van den Bergh and Sher on four plates of M67.

Bergh are systematically higher than those by Sher; that is to say the latter author was more conservative in his judgment of faint markings on the plate. Most of the counts which are reported in this paper have been made by Sher. Multiple counts of the same plate by Sher indicate that the root mean square deviation of two independent series of counts is 3.7 per cent.

An individual's counting limit is likely to vary somewhat over a period of time. To reduce, as much as possible, the effects of such systematic variations of the counting limit while counting stars on a single plate each cluster was divided into four quadrants and the quarter-rings thus formed were then counted in what was effectively a random order.

The basic data on each cluster were obtained by counting stars down to the plate limit on plates with different limiting magnitudes. In a number of cases these data were supplemented by counting only those stars brighter than a certain star of known magnitude, which was well above the plate limit. The latter data are considered to be of somewhat lower accuracy than the counts down to the plate limit.

The Number of Cluster Stars

To estimate the surface density of background stars, the area which was counted in each case extended well beyond the boundary of the cluster. A "rule of thumb" was to choose the background area roughly equal to the cluster area, but this precept was not followed rigidly.

Suppose that the adopted background area, A_b, contains N_b stars, then the density of background stars, σ_b, is

$$\sigma_b = \frac{N_b}{A_b} \tag{1}$$

Let there be $N(r_n)$ stars in the nth ring within the cluster, then the number of cluster stars within the ring is

$$N_c(r_n) = N(r_n) - A(n)\,\sigma_b \tag{2}$$

where $A\ (n)$ is the area of the nth ring.

Mean errors were associated with each determination of the number of cluster stars. These errors were obtained in the following way:
Let

ϵ_c = mean error of the number of cluster stars

ϵ_1 = mean error of the number of background stars within the area of the cluster, due to the uncertainty in the surface density of background stars, σ_b

ϵ_2 = error due to the statistical fluctuations of the number of background stars, themselves, within the cluster
then

$$\epsilon_c^2 = \epsilon_1^2 + \epsilon_2^2 \tag{3}$$

in which

$$\epsilon_1^2 = N_b \frac{A_c^2}{A_b^2} \quad \text{and} \quad \epsilon_2^2 = N_b \frac{A_c}{A_b}$$

where A_b is the background area and A_c is the cluster area. It should be emphasized that these errors do not take into account the uncertainties in the adopted limiting magnitudes or the uncertainties which might be introduced by irregular absorption over the background or cluster areas. Most of the clusters which will subsequently be discussed were selected for observation because they appeared projected on a relatively smooth field of background stars.

Determination of the Limiting Magnitudes

(a) Standard Sequences

Photoelectric sequences and (or) photographic transfers were used to establish a standard sequence in or near each cluster. The photographic magnitudes of the sequence stars were determined with the Eichner photometer of the California Institute of Technology. All magnitudes were transformed to the P system by means of the relation (Allen 1955).

$$P - V = 1.10\,(B - V) - 0.18 \tag{4}$$

Details on individual magnitude sequences are given below:

NGC 188: A photoelectric magnitude sequence to magnitude 17.2 was kindly supplied by Dr. Sandage. As NGC 188 lies less than 5° from the pole two transfer plates were taken, with both the cluster and the North Polar Sequence appearing on the same 14 × 14 inch plate. These transfers were used to set up a sequence in the cluster that included fainter stars than those in the photoelectrically obtained sequence. No significant deviations were found in the magnitude range where the two sequences overlap.

NGC 436, NGC 457, NGC 559, NGC 581, NGC 663, Trumpler 1: A photoelectric sequence by Pesch (1959) down to magnitude 14.6 was used. The sequence was extended by means of a photographic transfer to SA 51 in which Dr. Baum had established a photoelectric sequence which he kindly made available to us.

NGC 1907, NGC 1960: A magnitude sequence was set up by means of two photographic transfers to SA 51. No systematic differences between this sequence and sequences set up by Johnson and Morgan (1953) to $m_{pg} = 12.7$ and Cuffey (1937a) to $m_{pg} = 16.6$ were found.

NGC 2099: The magnitude sequence depends on one photographic transfer to SA 51.

NGC 2141, NGC 2194: The magnitude sequence depends on two photographic transfers to SA 51. Comparison of our sequence with one set up by Cuffey (1943) in NGC 2194 indicates a systematic difference in the sense m (Cuffey) $- m$ (adopted) $= 0.08$. Cuffey's sequence extends to magnitude 16.6.

NGC 2158: A photoelectric sequence in this cluster down to magnitude 20.0 was kindly made available to us by Dr. Arp.

NGC 2362: A photoelectric sequence down to magnitude 15.1 has been obtained in this cluster by Johnson and Morgan (1953). The sequence was extended to fainter magnitudes by means of two transfers to SA 57 in which a photoelectric sequence had been set up by Baum. The photographic transfers to this cluster are rather unsatisfactory since they were affected by fogging due to the lights of San Diego.

NGC 2477: A sequence by Miss Sawyer (1930), which is probably of rather low accuracy, was used.

NGC 2506, NGC 2539: The adopted magnitude sequences depend on two photographic transfers to SA 57.

NGC 2682: A photoelectric sequence down to magnitude 17.0 by Johnson and Sandage (1955) was extended to fainter magnitudes by means of two photographic transfers to SA 51. The transfer magnitudes were reduced by 0.2 magnitudes to bring them into agreement with the photoelectric sequence.

NGC 7789: A photoelectric sequence (Burbidge and Sandage 1958) down to magnitude 17.3 was kindly supplied by Dr. Sandage. This sequence was extended by means of two transfers to SA 68. The transfer magnitudes were shifted by 0.78 magnitudes to bring them into agreement with the photoelectric data. This large zero point error is probably due to the fact that the cluster was rather far west at the time of observation so that the plates may have been affected by twilight.

IC 361: The adopted magnitude sequence depends on two photographic transfers to SA 57.

In some cases the number of standard stars in a given magnitude interval was rather small. In such cases the magnitudes of additional stars were interpolated by measuring image diameters.

(*b*) *Determination of the plate limits*

The provisional limiting magnitude of each plate was determined from the standard sequence on that plate. Let m_i and m_j be the magnitudes of two adjacent stars of this sequence. If star i was visible but star j was not, then $\frac{1}{2}(m_i + m_j)$ was adopted as the provisional limiting magnitude of the plate. Sometimes the appearance of the images suggested that this limiting magnitude was too bright, or perhaps, too faint and the simple average, accordingly, was reduced or increased slightly. In the case of transfer plates it was assumed that the limiting magnitude in the selected area was equal to that in the cluster.

The limiting magnitudes obtained in this manner are unsatisfactory on two counts:

(1) The limiting magnitude is an interpolation between two limits m_i and m_j which in a representative sequence might differ by 0.3 magnitudes.

(2) No account is taken of possible fluctuations in the sensitivity of the photographic emulsion as a function of position on the plate. Clearly such variations might affect the visibility or invisibility of a certain sequence star.

The provisional limiting magnitudes were therefore adjusted by requiring them to fulfil the condition that the background count, $N_b(m)$ must be a smoothly increasing function of the limiting magnitude. Experience shows that the effective counting limit lies somewhat above the actual plate limit. From a comparison of the luminosity function of the inner region of M67 derived in this paper, with that obtained by Johnson and Sandage (1955) it was estimated that the effective counting limit is 0.5 magnitudes brighter than the actual plate limit. This correction was applied to the limiting magnitude of all counts down to the plate limit. The magnitudes in Tables I and II (see p. 220 to p. 235) therefore refer to the actual limiting magnitude of the counts and not to the plate limit itself.

TABLE III
BASIC DATA ON CLUSTERS

Cluster	$m-M_{pg}$	$m-M_o$	Distance	Age
NGC 188	10.5	10.5	1250 pc	old
NGC 436	13.7:	11.7:	2200:	young
NGC 457	14.3	12.3	2900	young
NGC 559	14.5:	11.7:	2200:	young
NGC 581 (M103)	13.9	11.9	2400	young
NGC 663	15.3	12.1	2600	young
NGC 1907	13.1::	11.1::	1650::	young
NGC 1960 (M36)	11.5	10.5	1250	young
NGC 2099 (M37)	11.1	10.7	1400	intermediate
NGC 2141	—	—	—	intermediate?
NGC 2158	14.8	13.4	4800	intermediate
NGC 2194	12.9:	10.4:	1200:	intermediate
NGC 2362 (τ CMa)	11.2	10.8	1450	young
NGC 2477	10.5::	—	—	intermediate
NGC 2506	—	—	—	intermediate?
NGC 2539	10.5	9.4	750	intermediate
NGC 2682 (M67)	9.8	9.5	800	old
NGC 7789	12.5	11.4	1850	intermediate
IC 361	—	—	—	intermediate?
Trumpler 1	14.2:	11.7:	2200:	young

NOTES ON TABLE III

NGC 188: Modulus obtained by fitting Sandage's provisional main sequence to the zero-age main sequence. Zero reddening was assumed.

NGC 436: True distance modulus taken from Bodén (1951). Absorption assumed to be same as that measured in the nearby cluster NGC 457 by Pesch (1959).

NGC 457: Data from Pesch (1959).

NGC 559: Data derived from Hiltner's (1956) observations of H.D. 8768 and H.D. 9105 using Johnson's (1959) intrinsic colours.

NGC 581: From Kruŝpán (1959). Hiltner's (1956) data on B.D. +59°273 confirm Kruŝpán's estimate of the reddening.

NGC 663: Data derived from Hiltner's (1956) observations of B.D. +60°331, 333, 339, 343 using Johnson's (1959) intrinsic colours.

NGC 1907: Distance and reddening were obtained under the assumption that the cluster is physically associated with nearby OB stars. The data for these OB stars were taken from Hiltner (1956).

NGC 1960: Data from Johnson (1957).

NGC 2099: Apparent modulus obtained by assuming the red giants in this cluster (Lindblad 1954) to have the same M_{pg} as those in the Hyades and Praesepe.

NGC 2158: Modulus obtained by fitting the colour-magnitude diagram given by Cuffey (1937b) to that of NGC 7789. The cluster-reddening was estimated by comparing provisional photoelectric magnitudes and colours obtained by Arp for some stars on the red giant branch with those obtained by Burbidge and Sandage (1958) in NGC 7789.

NGC 2194: Data from Cuffey (1943).

NGC 2362: Data from Johnson (1957).

NGC 2477: Measurements of the diameters of stellar images on red and blue plates indicate that the cluster colour-magnitude diagram is possibly intermediate between those of NGC 752 and M67. The cluster main sequence terminates at about $m_{pg} = 13.0$. Assuming this to correspond to $M_{pg} = +2.5$ one obtains $m - M_{pg} = 10.5$.

NGC 2539: Modulus obtained by comparing the cluster red giants (Zug 1933) with those in the Hyades and Praesepe. Absorption estimated by assuming $A_{pg} =$ 0.24 cosec b.

NGC 2682: Data from Johnson and Sandage (1955).

NGC 7789: Data from Burbidge and Sandage (1958).

Trumpler 1: Modulus from Kruŝpán (1959). Hiltner's (1956) colour excess for B.D. +60°274 is consistent with the absorption used by Kruŝpán.

THE LUMINOSITY FUNCTIONS OF CLUSTERS

(1) Old Galactic Clusters: NGC 188, NGC 2682 (M67)

NGC 188 and M67 are the two oldest known galactic clusters. Both clusters are located at intermediate galactic latitudes and are therefore particularly well suited for a determination of their luminosity functions. M67 appears projected on a very smooth stellar background.

Some faint emission and reflection nebulosity is visible in the vicinity of NGC 188 and star counts indicate some irregularities in the stellar background. As a result the luminosity function of NGC 188 is probably less accurate than that of M67. The luminosity functions of NGC 188 and M67 are shown on pages 236 and 237 respectively. Comparison of these two figures shows that the luminosity functions of both clusters exhibit a number of points of similarity. The integral luminosity functions of NGC 188 and M67 show a sudden increase in slope at $m_{pg} \simeq 15.6$ ($M_{pg} \simeq +5.1$) and $m_{pg} \simeq 13.3$ ($M_{pg} \simeq +3.5$) respectively corresponding to the termination points of the cluster main sequences. In both clusters the integral luminosity function has the largest slope (maximum of the differential luminosity function) less than one magnitude below the termination point of the main sequence. Below this maximum the luminosity functions decrease continuously down to the limits of observation. Comparison of the luminosity functions for the entire cluster with those for the inner region of each cluster shows that the brightest and hence most massive stars are more strongly concentrated towards the cluster nuclei than are the faintest least massive stars. Such an effect would be expected on dynamical grounds since both clusters are considerably older than their respective times of relaxation.

Table IV gives for both clusters the distance from the galactic plane, Z, the radius containing half of the cluster mass in projection, $r_{\frac{1}{2}}$, the largest distance to which the cluster could be traced, r_m, the extrapolated total cluster mass, $\mathfrak{M}$, the extrapolated total number of cluster stars, N, and the cluster relaxation time, τ, computed by means of an equation recently given by King (1959).

TABLE IV

Data on NGC 188 and M67

Cluster	Z	$r_{\frac{1}{2}}$	r_m	$\mathfrak{M}$	N	τ
NGC 188	+ 500 pc.	6.5′ = 2.4 pc.	20′ = 7.2 pc.	900$\mathfrak{M}_\odot$	1200:	1.2×10^8 y.
M67	+ 450	9.4 = 2.2	28 = 6.5	800	1000:	1.0×10^8

The mass-luminosity law tabulated by Schmidt (1959) was adopted to determine the total cluster mass. Stars which have evolved from the main sequence were assigned masses of 1.0 and 1.2 $\mathfrak{M}_\odot$ respectively in NGC 188 and M67. The mass in the form of white dwarfs was assumed to be 50$\mathfrak{M}_\odot$ in NGC 188 and 40$\mathfrak{M}_\odot$ in M67. The extrapolated total number of cluster stars, N, is considerably less accurate than the extrapolated total cluster mass $\mathfrak{M}$.

(2) Galactic Clusters of Intermediate Age: NGC 2099 (M37), NGC 2141, NGC 2158, NGC 2194, NGC 2477, NGC 2506, NGC 2539, NGC 7789, IC 361.

The luminosity functions of clusters of intermediate age (pages 238 to 246) show a number of interesting differences. Some of these differences are due to evolutionary effects, i.e. differences in the shapes of the red giant branches of the cluster colour-magnitude diagrams. In other clusters the differences are due to genuine differences in the cluster main sequence luminosity functions.

In the clusters NGC 2158 (p. 240) and NGC 7789 (p. 245) the slope of the integrated luminosity functions changes abruptly at $m_{pg} \simeq$ 17.0 ($M_{pg} \simeq +2.2$) and $m_{pg} \simeq 14.0$ ($M_{pg} \simeq +1.5$) respectively. This change in slope corresponds to the termination point of the cluster main sequence and to a concentration of red giants at the beginning of the cluster giant branch. The same explanation may also account for the sudden change in slope near $m_{pg} \simeq 17.7$ in the rich cluster NGC 2141 (p. 239), for which the distance modulus is unfortunately unknown. A similar explanation may account for the change in slope of the integral luminosity function of NGC 2506 (p. 243) near $m_{pg} \simeq$ 15.5 for which the distance modulus is also unknown.

The figure on p. 238 shows that the main sequence luminosity function of NGC 2099 (M37) has a flat maximum between the termination point of the cluster main sequence near $M_{pg} = 0$ and $M_{pg} = +4$. For fainter stars the luminosity function appears to decrease gradually. The main sequence luminosity functions of NGC 2477 (p. 242), NGC 2506 (p. 243) and NGC 2539 (p. 244), also seem to decrease slightly towards fainter magnitudes. The main sequence luminosity function of NGC 7789 (p. 245) appears to remain approximately constant over the range $+2.5 < M_{pg} < +5.5$. On the other hand the luminosity function of NGC 2194 (p. 241) seems to increase down to the limit of observation at $M_{pg} = +6$.

The data gave some indication that the brightest stars in NGC 2099 (M37), NGC 2194 and IC 361 are more concentrated towards the cluster nucleus than are the fainter stars.

(3) Young Galactic Clusters: NGC 436, NGC 457, NGC 559, NGC 581 (M103), NGC 663, NGC 1907, NGC 1960 (M36), NGC 2362 (τ CMa), Trumpler 1.

Young galactic clusters, which have only recently been formed from the interstellar gas, are usually located at low galactic latitudes. They, therefore, appear projected on a rich stellar background, which, due to the effects of absorbing interstellar clouds, is often quite irregular. As a result the luminosity functions of young galactic clusters are less reliable than those for the clusters of intermediate age, which have been discussed previously. Only in the case of the clusters NGC 436, NGC 457 and NGC 2362 was the background sufficiently homogeneous to determine the luminosity function in the usual manner.

For the other clusters it could, however, be assumed that the background was reasonably uniform over the two innermost rings. For these clusters only $f\phi(M)$ could be determined, in which f is an unknown constant which is smaller than one and $\phi(M)$ is the luminosity function of the entire cluster.

Let $N(r_n,m)$ be the total number of stars brighter than m in ring n and let $N_c(r_n,m)$ be the number of cluster stars brighter than m in ring n, then

$$N_c(r_n,m) = N(r_n,m) - \sigma_b(m)\, A(n) \tag{5}$$

in which $\sigma_b(m)$ is the surface density of background stars brighter than m and $A(n)$ is the area of ring n. Since we are dealing with very young clusters, which have ages smaller than their times of relaxation, it will be assumed that the radial density distribution of cluster stars is identical for *all* magnitudes. Equation (5) may then be written

$$K(n)\, N_c(m) = N(r_n,m) - \sigma_b(m)\, A(n) \tag{6}$$

in which $K(n)$ is the fraction of all cluster stars $N_c(m)$ in ring n. From equation (5) for rings 1 and 2 one obtains

$$f\, N_c(m) = \left[K(1) - \frac{K(2)}{3}\right] N_c(m) = N(1,m) - \frac{N(2,m)}{3} \tag{7}$$

This equation was used to determine the function $f\phi(M)$ for those clusters in which the absorption was judged to be relatively homogeneous over the nuclear region of the cluster.

The luminosity functions of the nine young clusters which were studied in the present investigation are shown on pages 247 to 250. The data indicate that the luminosity functions of young clusters differ from cluster to cluster. In the majority of the clusters the luminosity function appears to increase rapidly and then remains constant down to the limit of the observations. On the other hand the figures on p. 250 indicate that the clusters NGC 1907, NGC 1960 (M36) and NGC 2362 (τ CMa) appear to contain few if any intrinsically faint stars.

Star counts were made on the red prints of the Palomar Sky Survey in NGC 1907 and NGC 1960 to check the possibility that the apparent absence of faint cluster stars might be due to some peculiarity of the absorption in or near the nuclei of these clusters. Such absorption would of course be less effective in the red than in the blue. The results of the counts on the Sky Survey red prints are shown as open circles on p. 250 and seem to agree with the results obtained from the blue plates. Due to the fact that interstellar absorption is smaller in the red than in the blue, and because the faintest cluster stars are intrinsically red, the counts on the red prints should reach even fainter cluster stars than those recorded on the blue plates. It is therefore concluded that the absence of intrinsically faint stars in NGC 1907 and NGC 1960 (M36) is probably real. The possibility that the least massive stars in such very young clusters are still non-luminous, should of course, be kept in mind.

It is of some interest to note that if ϕ Cas is a member of NGC 457 (Pesch 1959), then the cluster contains stars with a brightness range of at least 15 magnitudes. On the other hand the main sequences of NGC 1907 and NGC 1960 (M36) only appear to be populated over a range of about 7 magnitudes.

The Radial Density Distribution of Cluster Stars

From the counts of stars in rings centred on the cluster nucleus the radial density distribution of cluster stars could be determined for the majority of the clusters contained in the present programme. The results are shown in figure 2, in which the fraction of all cluster stars $F(r/r_{\frac{1}{2}}^*)$ within radius r is plotted as a function of $r/r_{\frac{1}{2}}^*$ in which $r_{\frac{1}{2}}^*$ is the radius containing half of the cluster stars in projection. A cluster in which cluster stars could be traced out to a distance of n rings is represented in the figure by n points. The figure shows that the radial density distributions of all clusters which have been investigated are essentially similar. The scatter of the points for the outer regions of clusters may be largely due to the uncertainties inherent in the observations. The data for the high latitude clusters NGC 188 and M67 and the very rich cluster NGC 7789, which are believed to be more accurate than those for the other clusters, are given in Table V (the points for these clusters are shown as large dots in figure 2).

TABLE V

FRACTION OF ALL CLUSTER STARS $F(r/r_{1/2}^*)$ WITHIN RADIUS $r/r_{1/2}^*$

NGC 188

$r/r_{1/2}^*$	0.00	0.44	0.87	1.30	1.74	2.17	2.61	3.04
F	0.00	0.17	0.43	0.65	0.77	0.86	0.95	1.00

NGC 2682 (M67)

$r/r_{1/2}^*$	0.00	0.29	0.59	0.88	1.18	1.47	1.76	2.06	2.35	2.65	2.94
F	0.00	0.10	0.28	0.43	0.58	0.71	0.80	0.86	0.93	0.96	1.00

NGC 7789

$r/r_{1/2}^*$	0.00	0.34	0.69	1.03	1.38	1.72	2.07	2.41	2.76	3.10
F	0.00	0.11	0.34	0.51	0.68	0.81	0.90	0.94	0.98	1.00

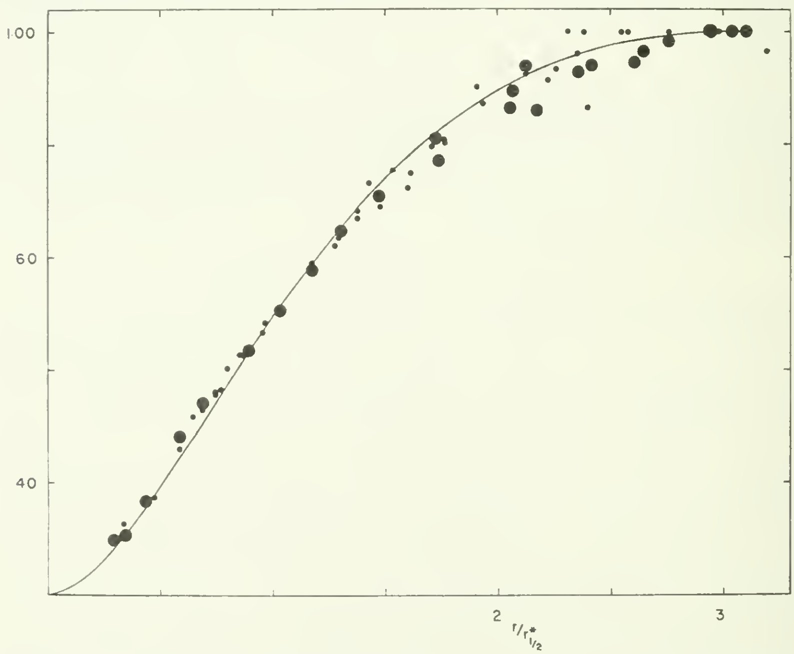

FIG. 2—Fraction of the total number of cluster stars $F(r/r_{1/2}^*)$ within a distance $r/r_{1/2}^*$ of the cluster centre. ($r_{1/2}^*$ is the radius containing half of the cluster stars in projection.) The curve shows $F(r/r_{1/2}^*)$ for an isothermal cluster.

In figure 2 a smooth curve shows $F(r/r_{\frac{1}{2}}^*)$ for an isothermal cluster with a cutoff at $\xi = 10$, which has been tabulated by Chandrasekhar (1942). The scale factor for the isothermal distribution was chosen such that $F = 0.5$ for $r = r_{\frac{1}{2}}^*$. Comparison of the observed points, with the curve representing an isothermal cluster, shows systematic deviations which are probably significant. For $r/r_{\frac{1}{2}}^* < 0.5$ the observed points lie above the isothermal curve and for $r/r_{\frac{1}{2}}^* > 0.5$ the observed points fall predominantly below it. The observations may be represented remarkably well by a stellar surface density, σ, of the following form

$$\frac{\sigma(r)}{\sigma(o)} = e^{-1.68r/r_{\frac{1}{2}}^*} \tag{8}$$

The data on the radii of the clusters contained in the present programme are given in Table VI.

TABLE VI

Cluster Radii Containing Half of the Cluster Stars in Projection

	$r_{\frac{1}{2}}^*$		D		$r_{\frac{1}{2}}^*$		D
NGC 188	8′.5	= 2.4 pc.	1250 pc.	NGC 2362	1′.6:	= 0.7:pc.	1450 pc.
NGC 436	1′.8:	= 1.2:pc.	2200:pc.	NGC 2477	6′.0	—	—
NGC 457	3′.8	= 3.2 pc.	2900 pc.	NGC 2506	4′.8	—	—
NGC 2099	8′.8	= 3.6 pc.	1400 pc.	NGC 2539	6′.7	= 1.5 pc.	750 pc.
NGC 2141	4′.1	—	—	NGC 2682	9′.7	= 2.3 pc.	800 pc.
NGC 2158	3′.6	= 5.0 pc.	4800 pc.	NGC 7789	8′.2	= 4.4 pc.	1850 pc.
NGC 2194	3′.7	= 1.3:pc.	1200:pc.	IC 361	3′.8	—	—

The data in the table may indicate a loose correlation between the radius containing half the total number of cluster stars and the stellar content of the clusters. NGC 2158 and NGC 7789, which are extremely rich, are seen to have larger than average radii.

Discussion of Results

Probably the most striking feature revealed by the luminosity functions shown on pages 236 to 250 is that significant differences exist between the luminosity functions of individual galactic clusters. Some of these differences may be explained in terms of the effects of stellar evolution on the positions of cluster stars in the Hertzsprung-Russell diagram. However, evolution of individual stars cannot account for the differences which are observed among the luminosity functions of unevolved main sequence cluster stars. The data on the luminosity functions of those clusters for which the observations extend below $M_{pg} = +5$ are summarized in Table VII. The data for the Hyades, Pleiades and Praesepe were taken from Sandage (1957).

TABLE VII
THE FAINT ENDS OF CLUSTER LUMINOSITY FUNCTIONS

Cluster	Limiting M_{pg}	$\phi(M_{pg})$
NGC 188	+10	Decreasing
NGC 436	+ 6	Constant?
NGC 457	+ 6	Constant?
NGC 559	+ 6	Constant?
NGC 581 (M103)	+ 6	Decreasing slightly?
NGC 663	+ 5	Decreasing slightly?
NGC 1907	+ 7	Decreasing
NGC 1960 (M36)	+ 9	Decreasing
NGC 2099 (M37)	+ 8	Decreasing slightly
NGC 2194	+ 6	Increasing
NGC 2362 (τ CMa)	+ 9	Decreasing
NGC 2539	+ 8	Decreasing slightly
NGC 2682 (M67)	+11	Decreasing
NGC 7789	+ 6	Constant
Trumpler 1	+ 6	Constant?
Hyades	+ 7	Constant
Pleiades	+10	Decreasing slightly
Praesepe	+ 7	Constant

Table VII shows that, with only one exception, the faint ends of the luminosity functions of galactic clusters either decrease or remain constant. This behaviour is in sharp contrast to that of the van Rhijn-Luyten luminosity function for field stars in the vicinity of the sun. Recent computations by Schmidt (1959) show that $\phi(M_{pg})$ for field stars begins to increase sharply at $M_{pg} = +5$. The present observations show that such an increase does not, in general, occur in the luminosity functions of galactic clusters.

In the case of very old clusters like NGC 188 and M67 it might be assumed that the difference between the cluster luminosity functions and the van Rhijn-Luyten luminosity function is due to the escape of faint cluster stars (van den Bergh 1957). However, the relaxation times of these clusters (see Table IV) are so long that it now appears unlikely that the entire discrepancy could be accounted for in this way. The fact that faint stars appear to be almost absent in such young objects as NGC 1907, M36 and the τ Canis Majoris cluster could conceivably be accounted for by assuming that such faint stars have not yet contracted to a position near the main sequence. However, this appears unlikely in the light of Walker's (1956) observations of the extremely young cluster NGC 2264, which show that stars as faint as $M_{pg} = +8$ occur in that cluster. In any case neither of the two special hypotheses outlined above could account for the differences between the van Rhijn-Luyten luminosity function and the luminosity functions of galactic clusters of intermediate age.

The differences between the luminosity functions of galactic clusters on the one hand and the luminosity function of field stars on the other may be accounted for in a number of ways. It may be assumed that:

(1) There now exists a universal cluster luminosity function which is identical to the luminosity function of star creation during the last few million years and this luminosity function differs from the initial luminosity function of star creation in the galaxy.

(2) The luminosity function of galactic star clusters is not representative of the luminosity function of star creation. This presumably implies that the conditions under which star clusters are created are not representative of the conditions under which "average" stars in the galaxy were formed.

For a number of reasons, the second hypothesis appears more attractive than the first. If the first hypothesis were correct then, to account for the present luminosity function of field stars, one would have to assume that the luminosity function of star creation in the galaxy initially contained a much larger fraction of faint stars than it does now. This is equivalent to saying that the initial luminosity function of star creation must have been deficient in bright stars. According to current views on stellar evolution, the ejection of heavy elements, formed by nucleogenesis in bright stars, enriches the heavy element concentration in the interstellar gas. It is, therefore, difficult to see how the presumably rapid increase in the heavy element abundance during the first phase of the evolution of the galaxy could be understood if the luminosity function of star creation were initially deficient in massive stars.

The striking differences between the luminosity functions of individual galactic clusters makes it difficult to believe in the universality of the luminosity function of star creation. It would appear to be more reasonable to assume that the differences between individual star clusters and also between star clusters on the one hand and field stars on the other are due to different physical conditions in the regions of star creation. Although our understanding of the processes by which stars are created from the interstellar gas is still very fragmentary, it appears likely that the resulting spectrum of stellar masses will depend to some extent on the prevailing gas density, temperature and turbulent velocity and perhaps also on the prevailing strength and configuration of the magnetic field.

The conclusion that the luminosity function with which stars are created depends on the physical conditions prevailing in the region of star formation implies that it is not possible to obtain a significant determination of the change in the rate of star formation with time by comparing the present main sequence luminosity function of bright field stars with the bright ends of cluster luminosity functions. Assuming the dependence of the rate of star formation, $f(t)$, on the gas density ρ, to be given by

$$f(t) \sim \rho^n \tag{9}$$

Schmidt (1959) obtains $n = 1$ to 2 from a comparison of the main sequence luminosity function of bright field stars with a "mean" luminosity function of bright stars in young clusters. On the other hand he finds that a comparison of the distribution of young stars and interstellar gas perpendicular to the galactic plane yields $n = 2$ to 3. The present investigation suggests that this discrepancy may be due to the fact that it is not legitimate to assume that the luminosity functions of galactic clusters are identical to the general luminosity function of star formation.

(Concluded on page 251)

TABLES AND FIGURES

Information concerning the arrangement of the tabular material and figures is given below.

Table I - Star Counts

The table contains the actual number of stars counted per ring down to each limiting magnitude. Limiting magnitudes marked by an asterisk refer to counts of stars brighter than a star of that magnitude. Limiting magnitudes not so marked refer to counts to the plate limit. Uncertain limiting magnitudes are followed by a colon. Limiting magnitudes followed by the letters B or R refer to counts on the blue or red prints of the Palomar Sky Survey. A vertical line in the tables indicates the adopted boundary between the cluster and background areas. In NGC 2158 and NGC 7789 numbers in parenthesis are counts corrected for overlapping images in the crowded cluster nuclei. In NGC 2158 numbers preceded by a minus sign give the number of background stars in the quadrant containing the nearby cluster M35. These were subtracted from the total number of stars in each ring to give the adopted background.

Table II - Integral Luminosity Functions

The table gives the total number of cluster stars N(m) down to each limiting magnitude as determined from the star counts in Table I. For most clusters the data are given separately for the inner region of the cluster, in which the cluster luminosity function is less affected by uncertainties in the adopted background level, than is the luminosity function of the entire cluster. For a number of young clusters only f N(m) is given in which f is an unknown constant which is smaller than one. In the case of NGC 2362 the inner half ring was excluded because the data are affected by the bright star τ CMa which is in the centre of the cluster.

Figures

The following figures give the integral luminosity functions (below) and differential luminosity functions (above) for the clusters contained in the present programme. The data for the inner cluster region are represented by the lower curve (scale on right) and solid histogram. The data for the entire cluster are given by the upper curve (scale on left) and the open histogram. Data obtained from the red prints of the Palomar Sky Survey are shown as open circles.

TABLE I - STAR COUNTS

NGC 188

m_{pg} \ Ring	1	2	3	4	5	6	7	8	9	10
9.90*	0	0	1	1	1	1	0	2	1	0
12.02*	0	1	1	4	3	6	3	4	2	6
13.15*	2	7	5	12	2	9	4	8	5	15
13.40	3	4	6	8	5	11	5	12	9	16
14.17*	7	22	12	19	10	20	20	20	24	31
14.71*	13	26	19	24	19	39	32	45	43	47
15.21*	21	46	30	29	22	46	42	48	47	59
15.59*	28	63	40	41	27	53	50	64	59	71
16.52*	75	171	124	110	81	111	93	135	116	148
17.00	86	159	138	129	104	135	131	161	160	180
17.23*	98	193	145	140	124	150	148	176	179	199
17.60	106	212	180	176	156	198	200	219	226	252
17.65	109	206	183	179	155	189	186	218	228	269
17.80*:	120	234	202	185	187	227	226	236	268	315
18.15:	114	226	213	190	196	225	236	250	284	333
18.40:	122	238	221	219	206	255	256	283	316	376
20.00:B	174	314	336	341	370	444	465	506	582	616
R	179	330	390	365	416	479	545	577	663	668

NGC 436

m_{pg} \ Ring	1	2	3	4	5
9.68*	0	0	0	0	0
10.35*	0	1	0	0	2

NGC 457

m_{pg} \ Ring	1	2	3	4	5	6	7
5.77*	0	1	0	0	0	0	0
7.53*	0	2	0	0	0	0	0

11.82*	5	1	0	6	2
13.14*	13	2	2	11	7
14.50	19	8	15	22	20
14.90	34	17	26	41	32
15.45	41	23	34	54	51
16:00:	48	33	44	68	74
16.25	51	43	52	91	104
16.45	60	58	61	90	116
20.30:B	278	410	677	933	1201
R	277	493	739	932	1151

9.68*	1	5	1	1	0	0	1
10.35*	4	7	5	1	2	0	2
11.82*	12	18	9	3	4	0	4
13.14*	21	26	14	7	6	1	8
14.50	43	53	25	30	36	29	48
14.90	45	65	26	41	42	39	55
15.45	53	81	41	55	53	62	76
16.25	71	112	75	99	89	109	128
16.45	70	117	92	104	97	123	149
20.30:B	260	476	659	831	1084	1231	1437

	NGC 559		NGC 581		NGC 663		Tr 1	
Ring	1	2	1	2	1	2	1	2
m_{pg}								
9.68*	0	0	1	1	0	1	0	0
10.35*	0	0	2	1	0	5	0	0
11.82*	0	2	13	3	5	14	6	0
13.14*	3	3	23	8	20	26	8	2
14.50	11	3	46	27	38	41	30	17
14.90	19	6	52	38	45	57	34	26
15.45	29	21	52	54	55	97	45	36
16.00:	38	28	58	74	61	106	48	40
16.25	51	40	69	89	69	128	61	47
16.45	59	53	66	100	75	135	63	58
16.85*:	85	115	83	166	82	159	78	109
18.60:	-	-	125	277	133	264	116	171
19.30:	-	-	195	432	154	349	156	326
20.30:B	259	426	280	675	227	456	242	451
R	318	651	282	697	250	610	297	621

TABLE I (continued)

Ring / m_{pg}	NGC 1907: 1	NGC 1907: 2	NGC 1960: 1	NGC 1960: 2
7.53*	0	0	0	0
9.08*	0	0	6	2
9.58*	0	0	7	3
10.51*	2	0	9	6
11.55	4	2	13	9
12.25	5	3	17	13
13.70	16	13	28	31
14.35	35	27	39	44
15.00	50	47	43	53
15.25	49	54	45	63
15.60	66	72	48	67
16.20	75	92	50	76
17.50	95	140	61	107
18.20	105	159	67	135
18.40	96	183	-	-
18.40	94	171	-	-
18.70	108	194	66	149
19.10	116	232	78	169
20.50:B	-	-	147	377
20.60:B	182	368	-	-
R	189	413	183	477

NGC 2099 (M37)

Ring / m_{pg}	1	2	3	4	5	6	7	8	9	10	11
10.68*	3	0	1	0	0	1	1	1	3	8	1
11.72*	37	29	32	17	11	5	6	14	8	18	7

12.78*	79	73	66	41	34	19	17	27	23	31	19
13.60	97	118	87	59	63	58	39	69	58	74	52
13.65	92	107	95	63	68	59	45	75	65	82	64
14.00	118	132	123	88	108	87	71	105	90	118	104
14.15	108	137	119	97	112	96	90	106	120	133	116
14.50	124	153	146	130	139	125	125	149	168	160	176
14.65	127	161	158	138	158	146	144	167	186	181	191
15.55	145	216	229	199	231	231	266	279	297	326	344
17.40	182	331	374	418	485	537	624	666	753	849	886
17.95	192	374	432	507	585	711	762	875	909	1040	1148
18.20	202	368	455	582	675	771	877	958	1072	1180	1186
18.60	210	393	529	615	749	847	959	1074	1172	1353	1428
19.35	222	487	605	792	890	1117	1173	1379	1536	1604	1677

NGC 2141

m_{pg} \ Ring	1	2	3	4	5	6	7
12.35*	0	4	2	4	5	7	6
13.76*	3	13	18	19	27	23	27
14.89*	6	16	24	24	44	32	44
16.15	36	33	55	68	87	89	121
16.75	45	56	83	96	135	121	172
17.10	59	70	95	123	160	156	202
17.65	75	121	128	173	222	229	301
17.85	100	143	160	203	249	282	321
18.20	138	209	216	278	289	351	434
18.35	153	240	252	322	340	416	474
18.40	174	246	268	323	342	439	500
18.95	206	345	360	463	524	630	705
19.30	240	417	453	586	653	762	882
19.55:B	380	517	568	655	719	854	1059

TABLE I (continued)

NGC 2158

Ring / m_{pg}	1	2	3	4	5	6	7
10.69*	1	1	4	3	0	4	6
						-1	-4
12.85	8	8	16	15	21	24	39
						-8	-22
13.65	13	15	23	21	38	40	64
						-12	-30
14.00	9	20	30	27	51	53	81
						-18	-39
14.35	17	26	36	39	76	65	92
						-19	-37
15.35	28	33	67	71	113	113	150
						-30	-55
16.00	68	76	106	106	160	180	216
						-59	-85
16.70	92	109	145	152	213	244	317
						-80	-123
16.90	100	125	158	167	231	271	342
						-89	-124
18.00	281	262	270	302	381	453	597
	(286)	(264)	(271)	(303)		-156	-193
18.50	331	343	346	403	476	621	719
	(338)	(345)	(348)	(405)		-219	-221
19.00	474	493	442	525	618	773	946
	(495)	(500)	(447)	(529)		-268	-278
19.25	442	563	520	632	699	903	1024
	(469)	(577)	(528)	(640)		-286	-324

NGC 2194

m_{pg} \ Ring	1	2	3	4	5
10.72*	1	0	1	1	2
11.45*	0	1	2	2	2
11.75	12	7	10	10	16
11.80	14	9	16	8	19
12.35*	3	6	14	18	16
13.76*	24	20	31	40	35
14.89*	47	35	40	55	47
16.15	69	69	73	72	79
16.75	97	97	102	101	120
17.10	95	115	114	126	150
17.65	119	148	163	184	206
17.85	143	185	190	201	235
17.90	149	168	187	205	243
18.20	171	214	238	239	290
18.25	156	208	238	248	293
18.35	178	218	240	271	313
18.40	178	234	257	278	323
18.65	179	277	292	317	372
18.75	188	290	313	347	404
18.95	209	342	345	368	443
19.30	250	406	442	472	561
19.55:B	274	412	494	506	628

NGC 2362 (τ CMa)

m_{pg} \ Ring	$\frac{1}{2}$	1	$1\frac{1}{2}$	2	3
6.63*	1	0	0	0	1
7.61*	1	2	0	0	3

TABLE I (continued)

NGC 2362 (τ CMa) (continued)

Ring / m_{pg}	½	1	1½	2	3
8.83*	3	4	0	0	4
10.17*	9	8	3	0	4
11.21*	15	10	8	2	5
12.25*	15	17	13	1	14
13.40	18	23	16	8	13
14.80	24	27	21	11	27
16.00	25	33	31	22	60
17.50	24	45	59	51	137
18.45	33	60	89	105	262
18.75	30	72	102	110	286
20.00	34	106	169	183	551

NGC 2477

Ring / m_{pg}	1	2	3	4	5	6	7
10.1*	0	0	1	0	0	1	3
11.4*	1	4	5	3	4	6	10
13.1*	19	26	26	7	7	10	20
14.5*	86	121	113	94	85	51	64
15.9*	136	214	232	193	198	164	184
16.8*	169	282	292	263	260	232	294
18.0::	218	466	552	551	567	555	656

NGC 2506

Ring / m_{pg}	1	2	3	4	5	6	7
12.15*	3	2	3	1	5	7	8
13.00*	7	5	5	4	9	11	17
13.70*	18	12	14	13	17	24	30
15.05	86	65	51	58	86	92	116
15.50	84	81	66	74	87	101	120
15.85*	51	95	66	98	112	129	100
16.15	157	174	132	156	161	179	198
16.65	200	239	194	197	212	240	263
17.05	231	292	267	282	306	304	358
17.20*	269	401	340	399	463	443	511
18.00	292	460	422	493	547	597	640
18.05*:	302	517	466	552	551	639	740
18.40B	327	485	587	618	634	763	756
18.65	359	584	579	642	666	838	883

NGC 2539

Ring / m_{pg}	1	2	3	4	5	6	7	8	9
9.15*	0	0	0	1	0	0	1	0	0
10.90*	2	1	0	5	2	2	2	4	3
12.15*	10	18	10	13	5	5	10	8	6
13.00*	16	27	23	25	16	9	15	11	14
13.70*	21	44	33	42	30	30	38	29	30
15.05	25	53	49	68	58	54	68	57	66
15.50	34	73	71	93	90	91	.111	104	129
15.85*	37	85	81	112	119	112	132	124	118
16.15	43	100	101	130	135	149	185	149	216

TABLE I (continued)

NGC 2539 (continued)

Ring / m_{pg}	1	2	3	4	5	6	7	8	9
16.65	50	118	127	178	182	220	244	264	318
17.05	58	137	164	211	230	287	325	333	415
17.20*	69	162	217	262	324	377	441	464	532
18.00	75	187	247	340	400	476	547	603	705
18.05*:	84	192	268	336	409	480	557	578	710
18.65	103	248	343	454	571	669	811	864	1047

NGC 2682 (M67)

Ring / m_{pg}	1	2	3	4	5	6	7	8	9	10	11	12	13	14	15	16	17	18
9.78*	0	1	1	0	0	0	1	1	0	0	2	2	2	1	2	2	2	0
10.67*	5	6	4	0	1	0	2	1	3	1	4	3	3	4	3	3	7	1
11.10*	6	7	2	1	1	0	3	1	2	3	3	4	4	3	3	3	6	3
11.51*	8	11	5	3	2	0	3	4	2	3	4	5	3	5	5	4	7	3
11.83*	8	11	5	3	4	1	4	5	3	5	5	8	4	8	7	6	9	4
11.95	11	15	6	4	5	1	4	8	4	4	6	8	5	10	9	5	10	5
12.30*	12	24	8	4	5	3	7	8	4	7	9	11	7	9	11	8	16	8
13.25	20	30	15	7	18	13	10	16	14	23	12	21	18	17	24	18	27	15
13.60	28	44	22	15	25	20	14	18	21	24	24	28	20	24	30	16	26	17
14.30	40	76	38	37	36	30	26	27	33	31	30	34	30	33	37	28	49	26
14.60	42	87	47	57	42	39	32	35	41	34	30	40	33	40	45	37	53	36
15.45	53	89	62	73	59	49	52	45	46	45	47	52	50	55	64	49	75	65
16.30	56	119	74	100	75	75	61	67	67	71	66	74	74	91	94	79	104	84
16.90	65	129	89	108	96	86	76	85	81	83	81	87	95	98	114	98	130	110
17.70	69	130	109	122	111	108	96	99	107	108	118	114	125	127	156	134	162	151

18.55	75	146	130	133	130	124	121	127	130	137	148	156	145	165	204	172	209	208
19.25	78	149	143	165	151	151	149	157	162	177	182	198	183	208	261	241	251	282
19.30	74	158	136	160	142	148	147	157	166	172	181	196	198	211	263	231	276	260
19.40	80	161	145	165	152	152	160	157	179	176	187	192	198	213	270	236	287	270
19.85	79	169	160	173	180	175	172	193	195	214	211	231	228	254	310	294	327	337
20.65B	92	172	179	199	217	212	209	236	236	261	246	280	294	362	406	384	389	424

NGC 7789

Ring / m_{pg}	1	2	3	4	5	6	7	8	9	10	11	12
11.07*	1	2	1	5	3	1	6	7	7	5	8	14
12.68*	7	22	12	21	27	26	35	37	25	31	42	49
13.14*	10	24	16	19	26	22	39	36	33	28	38	68
13.88*	17	40	25	40	41	44	36	45	30	45	43	81
14.25	45	86	60	53	62	61	88	71	72	82	92	123
14.75	75	122	103	85	92	106	126	99	109	118	134	165
14.77*	46	92	83	92	91	99	114	114	93	99	104	155
15.09*	99	241	182	218	214	215	256	200	257	227	283	323
15.15	91	186	136	138	144	147	164	159	159	153	196	226
15.45	115	221	183	185	195	171	204	191	190	195	247	272
16.49*	159	346	341	350	391	365	463	433	487	450	515	608
17.26*	197	444	440	528	535	596	639	683	749	821	864	1007
17.60:	225	508	549	651	678	700	795	860	956	1032	1086	1250
	(238)	(526)	(558)	(660)	(685)	(706)	(802)					
18.00:	253	617	677	828	895	943	1072	1131	1274	1372	1511	1690
	(266)	(637)	(687)	(837)	(904)	(950)	(1080)					
18.10:	261	606	671	875	897	994	1068	1254	1326	1443	1581	1805
	(279)	(634)	(686)	(890)	(910)	(1006)	(1081)					
18.20:	272	720	742	941	1001	1105	1183	1355	1473	1683	1745	1943
	(305)	(762)	(763)	(961)	(1019)	(1121)	(1200)					
18.20:	290	686	754	938	1026	1079	1176	1363	1479	1586	1764	1961
	(309)	(717)	(770)	(953)	(1040)	(1091)	(1189)					

TABLE I (concluded)

IC 361

Ring / m_{pg}	1	2	3	4	5	6	7
14.60	3	9	8	11	18	28	27
15.50	11	14	17	25	38	52	50
15.80	23	19	25	43	43	60	65
16.15	40	28	26	59	55	83	78
17.10*	65	86	82	84	112	135	162
17.70	180	128	120	154	169	223	221
18.25	153	158	167	201	252	274	340
18.25	136	155	152	200	226	287	338
18.55	162	182	180	235	274	339	403
18.85	180	204	237	287	331	397	480
19.00	215	229	241	304	359	427	526
20.00:B	255	377	412	485	625	713	901
R	317	554	741	845	974	1266	1478

TABLE II - LUMINOSITY FUNCTIONS

NGC 188

m_{pg}	Inner Region Rings 1,2,3	Entire Cluster
9.90*	1 ± 0	1 ± 2
12.02*	0 ± 1	6 ± 5
13.15*	8 ± 1	13 ± 7
13.40	6 ± 2	6 ± 8
14.17*	29 ± 2	40 ± 12
14.71*	34 ± 3	42 ± 16
15.21*	70 ± 3	89 ± 17
15.59*	97 ± 3	116 ± 19
16.52*	300 ± 5	381 ± 27
17.00	295 ± 6	401 ± 31
17.23*	338 ± 6	466 ± 31
17.60	375 ± 7	559 ± 36
17.65	372 ± 7	521 ± 37
17.80*:	412 ± 7	597 ± 39
18.15:	400 ± 7	567 ± 40
18.40:	409 ± 8	581 ± 42
20.00:B	524 ± 10	807 ± 57
R	563 ± 11	873 ± 60

	NGC 436		NGC 457	
m_{pg}	Inner Region Ring 1	Entire Cluster	Inner Region Rings 1,2	Entire Cluster
5.77*	0 ± 0	0 ± 0	1 ± 0	1 ± 0
7.53*	0 ± 0	0 ± 0	2 ± 0	2 ± 0
9.68*	0 ± 0	0 ± 0	6 ± 0	8 ± 1
10.35*	0 ± 0	1 ± 1	11 ± 1	15 ± 2
11.82*	5 ± 1	5 ± 1	29 ± 1	38 ± 2
13.14*	12 ± 1	11 ± 2	45 ± 1	61 ± 3
14.50	16 ± 2	16 ± 4	82 ± 4	96 ± 9
14.90	19 ± 2	22 ± 5	94 ± 4	111 ± 10
15.45	34 ± 3	37 ± 6	111 ± 5	137 ± 12
16.00:	37 ± 3	43 ± 6	-	-
16.25	39 ± 4	47 ± 7	143 ± 7	199 ± 15
16.45	47 ± 4	67 ± 8	142 ± 7	204 ± 16
20.30:B	144 ± 12	153 ± 25	281 ± 23	406 ± 52
R	143 ± 12	233 ± 25		

m_{pg}	NGC 559 fN(m)	NGC 581 fN(m)	NGC 663 fN(m)	Tr 1 fN(m)
9.68*	0 ± 0	1 ± 0	0 ± 1	0 ± 0
10.35	0 ± 0	2 ± 1	-2 ± 1	0 ± 0
11.82*	-1 ± 1	12 ± 1	0 ± 2	6 ± 0
13.14*	2 ± 1	20 ± 2	11 ± 3	7 ± 1
14.50	10 ± 1	37 ± 3	24 ± 4	24 ± 3
14.90	17 ± 2	39 ± 4	26 ± 5	25 ± 3
15.45	22 ± 3	34 ± 5	23 ± 7	33 ± 4
16.00:	29 ± 4	33 ± 6	26 ± 7	35 ± 4
16.25	38 ± 4	39 ± 6	26 ± 8	45 ± 5

TABLE II (continued)

(cont'd) m_{pg}	NGC 559 fN(m)	NGC 581 fN(m)	NGC 663 fN(m)	Tr 1 fN(m)
16.45	41 ± 5	33 ± 7	30 ± 8	44 ± 5
16.85*:	47 ± 8	28 ± 9	29 ± 8	42 ± 7
18.60:	-	32 ± 11	45 ± 11	59 ± 9
19.30:	-	51 ± 14	38 ± 12	47 ± 12
20.30:B	117 ± 14	55 ± 17	75 ± 14	92 ± 14
R	101 ± 17	50 ± 17	47 ± 16	90 ± 17

m_{pg}	NGC 1907 fN(m)	NGC 1960 fN(m)
7.53*	0 ± 0	0 ± 0
9.08*	0 ± 0	5 ± 1
9.58*	0 ± 0	6 ± 1
10.51*	2 ± 0	7 ± 2
11.55	3 ± 1	10 ± 2
12.25	4 ± 1	13 ± 2
13.70	12 ± 2	18 ± 4
14.35	26 ± 3	24 ± 4
15.00	34 ± 5	25 ± 5
15.25	31 ± 5	24 ± 5
15.60	42 ± 6	26 ± 5
16.20	44 ± 6	25 ± 6
17.50	48 ± 8	25 ± 7
18.20	52 ± 8	22 ± 8
18.40	35 ± 9	-
18.40	37 ± 9	-
18.70	43 ± 9	16 ± 8
19.10	39 ± 10	22 ± 9
20.50:B	-	21 ± 13
20.60:B	59 ± 13	-
R	51 ± 14	24 ± 14

NGC 2099 (M37)

m_{pg}	Inner Region Rings 1,2,3	Entire Cluster
10.68*	2 ± 1	-6 ± 5
11.72*	93 ± 2	114 ± 9
12.78*	206 ± 4	274 ± 13
13.60	273 ± 6	383 ± 21
13.65	261 ± 6	367 ± 22
14.00	324 ± 8	482 ± 27
14.15	304 ± 8	443 ± 30
14.50	343 ± 10	524 ± 35
14.65	358 ± 10	572 ± 36
15.55	437 ± 13	709 ± 48
17.40	494 ± 21	823 ± 77
17.95	509 ± 24	961 ± 86
18.20	482 ± 25	1028 ± 90
18.60	508 ± 27	938 ± 97
19.35	552 ± 30	1253 ± 107

NGC 2141

m_{pg}	Inner Region Rings 1,2	Entire Cluster
10.72*	-	-
11.45*	-	-
11.75	-	-
11.80	-	-
12.35*	1 ± 2	0 ± 4
13.76*	7 ± 3	16 ± 7
14.89*	7 ± 4	12 ± 9
16.15	33 ± 6	48 ± 15
16.75	49 ± 8	72 ± 18
17.10	66 ± 8	95 ± 19
17.65	105 ± 10	132 ± 23
17.85	140 ± 11	193 ± 25
17.90	-	-
18.20	216 ± 12	319 ± 28
18.25	-	-
18.35	244 ± 13	370 ± 30
18.40	265 ± 14	390 ± 30
18.65	-	-
18.75	-	-
18.95	326 ± 16	473 ± 37
19.30	378 ± 18	582 ± 41
19.55:B	578 ± 19	844 ± 44

NGC 2194

m_{pg}	Inner Region Ring 1	Entire Cluster
10.72*	1 ± 0	0 ± 2
11.45*	-1 ± 1	0 ± 2
11.75	10 ± 1	14 ± 5
11.80	12 ± 1	24 ± 5
12.35*	1 ± 2	4 ± 5
13.76*	19 ± 2	33 ± 8
14.89*	41 ± 3	65 ± 9
16.15	60 ± 3	127 ± 12
16.75	83 ± 4	172 ± 12
17.10	78 ± 4	169 ± 16
17.65	95 ± 5	211 ± 18
17.85	116 ± 5	273 ± 20
17.90	121 ± 5	252 ± 20
18.20	138 ± 6	326 ± 21
18.25	122 ± 6	297 ± 22
18.35	141 ± 6	306 ± 23
18.40	140 ± 6	330 ± 23
18.65	136 ± 7	361 ± 25
18.75	141 ± 7	368 ± 26
18.95	158 ± 7	439 ± 27
19.30	185 ± 8	516 ± 30
19.55:B	203 ± 9	541 ± 31

NGC 2158

m_{pg}	Inner Region Rings 1,2	Entire Cluster
10.69*	1 ± 1	2 ± 4
12.85	9 ± 3	22 ± 10
13.65	14 ± 4	24 ± 14
14.00	12 ± 5	30 ± 16
14.35	21 ± 5	54 ± 18
15.35	21 ± 7	65 ± 24
16.00	88 ± 8	166 ± 29
16.70	121 ± 10	214 ± 34
16.90	136 ± 10	225 ± 36
18.00	394 ± 14	531 ± 48
18.50	483 ± 16	662 ± 55
19.00	736 ± 18	960 ± 62
19.25	753 ± 19	1084 ± 66

NGC 2362 (τ CMa)

m_{pg}	fN(m)
6.63*	0 ± 1
7.61*	1 ± 1
8.83*	3 ± 1
10.17*	10 ± 1
11.21*	16 ± 2
12.25*	26 ± 2
13.40	33 ± 3
14.80	37 ± 4
16.00	40 ± 5
17.50	48 ± 8
18.45	40 ± 11
18.75	57 ± 11
20.00	57 ± 15

NGC 2477

m_{pg}	Inner Region Rings 1,2	Entire Cluster
10.1*	0 ± 1	-3 ± 3
11.4*	2 ± 2	0 ± 6
13.1*	40 ± 2	54 ± 8
14.5*	188 ± 5	379 ± 16
15.9*	293 ± 8	610 ± 27
16.8*:	363 ± 10	717 ± 33
18.0::	483 ± 15	1093 ± 51

TABLE II (continued)

m_{pg}	NGC 2506 Inner Region Rings 1,2	NGC 2506 Entire Cluster	NGC 2539 Inner Region Rings 1,2,3	NGC 2539 Entire Cluster
9.15*	-	-	0 ± 0	0 ± 1
10.90*	-	-	1 ± 1	5 ± 4
12.12*	3 ± 2	-2 ± 6	33 ± 2	42 ± 6
13.00*	7 ± 2	1 ± 8	58 ± 3	84 ± 8
13.70*	21 ± 3	18 ± 11	79 ± 5	122 ± 12
15.05	116 ± 6	129 ± 21	89 ± 7	154 ± 17
15.50	128 ± 7	162 ± 22	109 ± 9	177 ± 22
15.85*	108 ± 7	183 ± 22	128 ± 9	247 ± 23
16.15	268 ± 9	387 ± 28	130 ± 12	218 ± 28
16.65	355 ± 10	518 ± 33	130 ± 14	214 ± 34
17.05	413 ± 11	688 ± 38	144 ± 16	229 ± 39
17.20*	511 ± 14	878 ± 45	161 ± 19	261 ± 45
18.00	546 ± 16	925 ± 51	138 ± 21	241 ± 52
18.05*:	589 ± 16	952 ± 54	175 ± 21	293 ± 52
18.40B	559 ± 17	1069 ± 57	-	-
18.65	656 ± 18	1037 ± 60	150 ± 26	210 ± 63

NGC 2682 (M67)

m_{pg}	Inner Region Rings 1,2,3	Entire Cluster
9.78*	1 ± 1	-2 ± 3
10.67*	14 ± 1	11 ± 4
11.10*	14 ± 1	13 ± 4
11.51*	23 ± 1	25 ± 5
11.83*	22 ± 1	26 ± 6
11.95	30 ± 2	36 ± 6
12.30*	41 ± 2	47 ± 7
13.25	59 ± 2	98 ± 10
13.60	87 ± 3	148 ± 11
14.30	143 ± 3	255 ± 13
14.60	163 ± 4	316 ± 14
15.45	186 ± 4	369 ± 17
16.30	222 ± 5	468 ± 21
16.90	250 ± 6	535 ± 23
17.70	264 ± 7	574 ± 27
18.55	294 ± 8	625 ± 30
19.25	297 ± 9	676 ± 34
19.30	295 ± 9	649 ± 35
19.40	312 ± 9	700 ± 35
19.85	320 ± 9	731 ± 38
20.65B	331 ± 10	770 ± 42

NGC 7789

m_{pg}	Inner Region Rings 1,2,3	Entire Cluster
11.07*	0 ± 2	-2 ± 9
12.68*	24 ± 5	55 ± 19
13.14*	31 ± 5	53 ± 20

TABLE II (concluded)

NGC 7789 (concluded)

m_{pg}	Inner Region Rings 1,2,3	Entire Cluster
13.88*	59 ± 5	100 ± 22
14.25	149 ± 7	216 ± 30
14.75	240 ± 8	381 ± 35
14.77*	170 ± 8	364 ± 32
15.09*	403 ± 12	811 ± 50
15.15	331 ± 10	601 ± 41
15.45	417 ± 11	737 ± 46
16.49*	621 ± 16	1313 ± 68
17.26*	696 ± 21	1350 ± 89
17.60:	841 ± 24	1661 ± 99
18.00:	937 ± 27	1886 ± 116
18.10:	909 ± 28	1857 ± 119
18.20:	1063 ± 30	1054 ± 126
18.20:	1037 ± 29	2083 ± 125

IC 361

m_{pg}	Inner Region Ring 1	Entire Cluster
14.60	1 ± 1	-5 ± 7
15.50	7 ± 2	-1 ± 10
15.80	18 ± 2	29 ± 11
16.15	33 ± 3	47 ± 12
17.10*	53 ± 3	119 ± 16
17.70	111 ± 4	234 ± 20
18.25	127 ± 5	259 ± 24
18.25	110 ± 5	231 ± 24
18.55	131 ± 6	267 ± 26
18.85	146 ± 6	322 ± 28
19.00	175 ± 6	352 ± 29
20.00:B	187 ± 8	445 ± 38
R	204 ± 11	654 ± 52

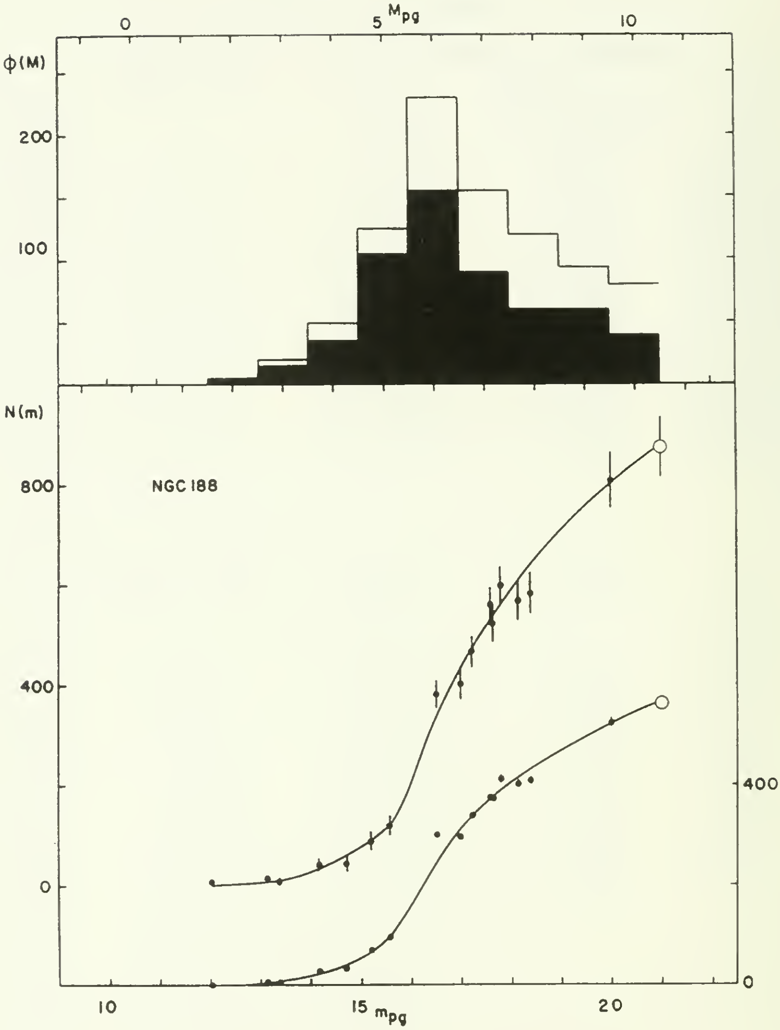
M_{pg}
0
5
10
$\phi(M)$
200
100
N(m)
800
400
0
NGC 188
400
0
10
15
20
m_{pg}

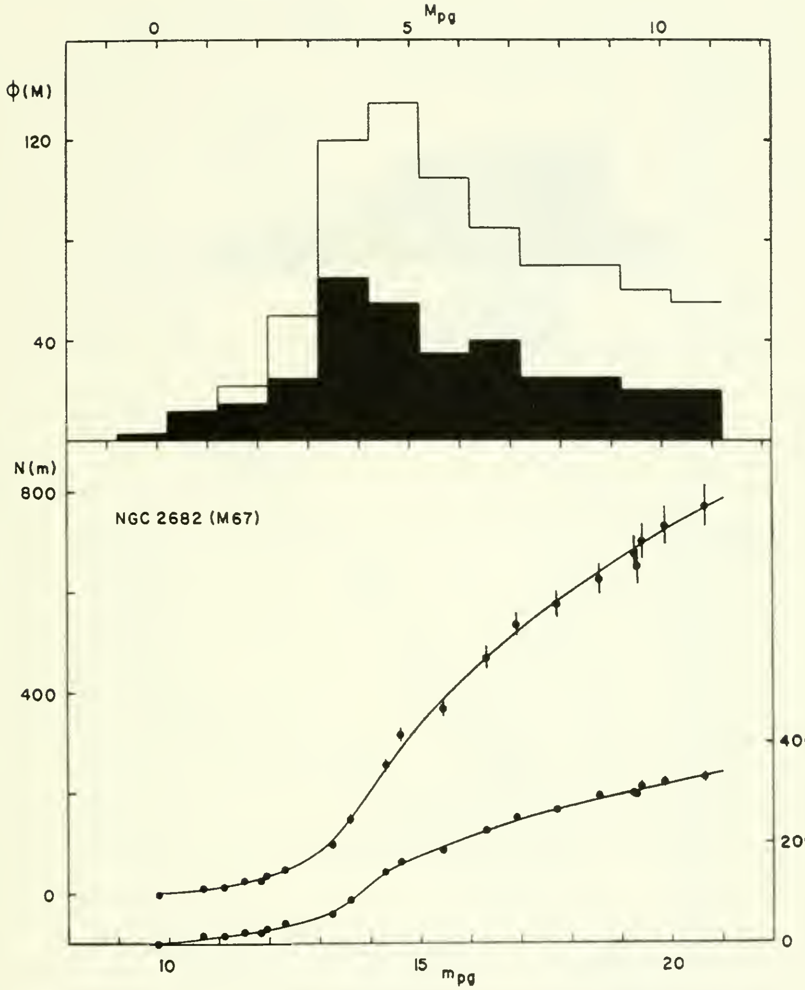
M_{pg}
0
5
10
$\phi(M)$
120
40
N(m)
800
400
0
NGC 2682 (M67)
400
200
0
10
15
m_{pg}
20

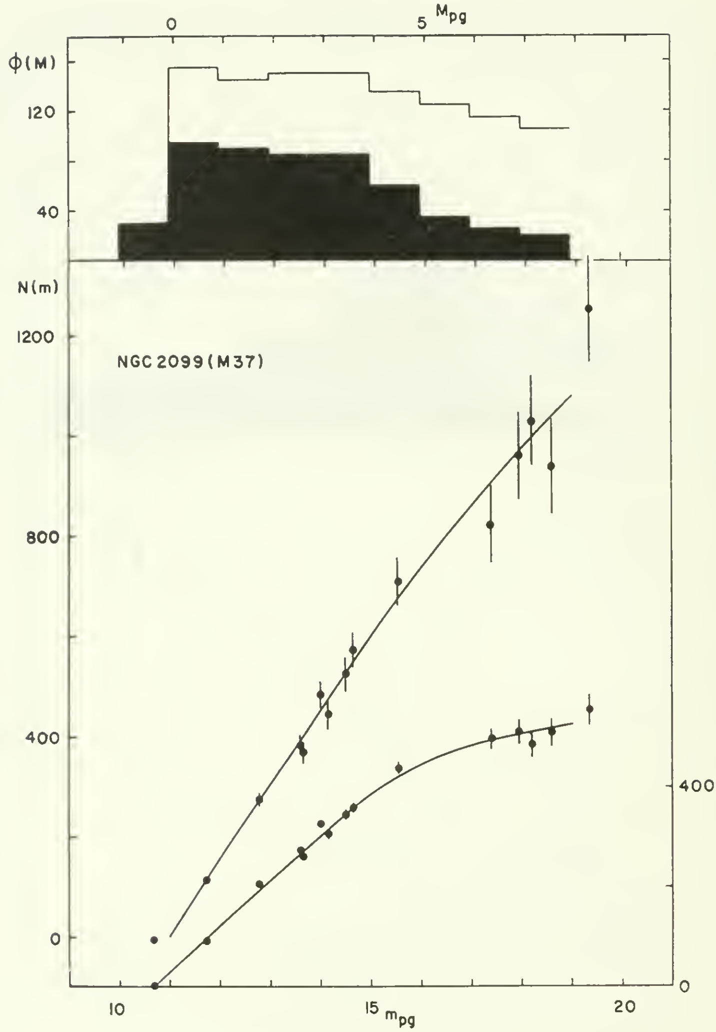
0
5 M_{pg}
$\phi(M)$
120
40
N(m)
1200
NGC 2099 (M37)
800
400
0
400
0
10
15 m_{pg}
20

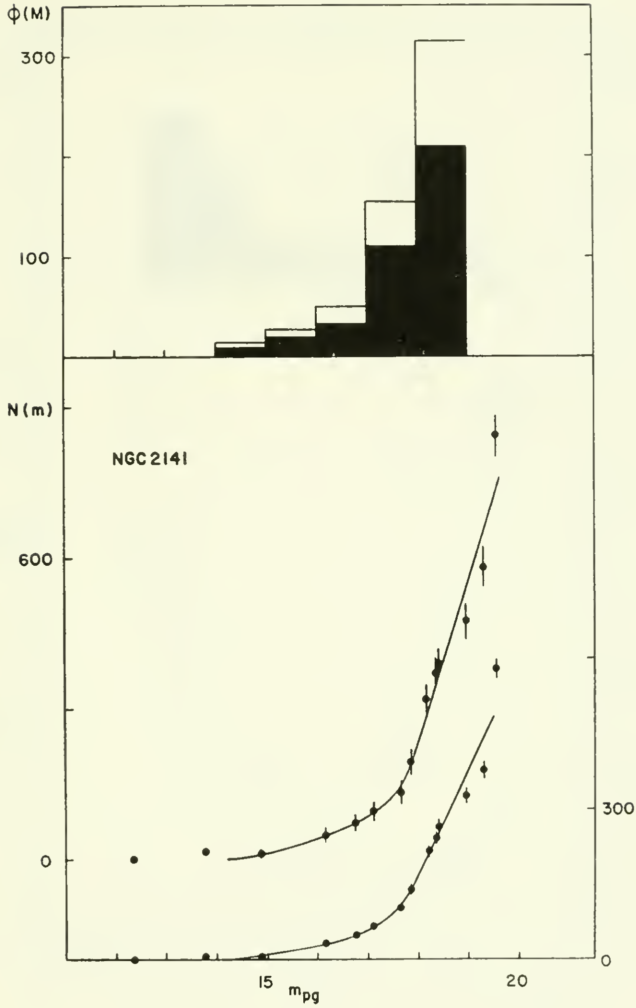

φ(M)
300
100
N(m)
NGC 2141
600
0
300
0
15
m_pg
20

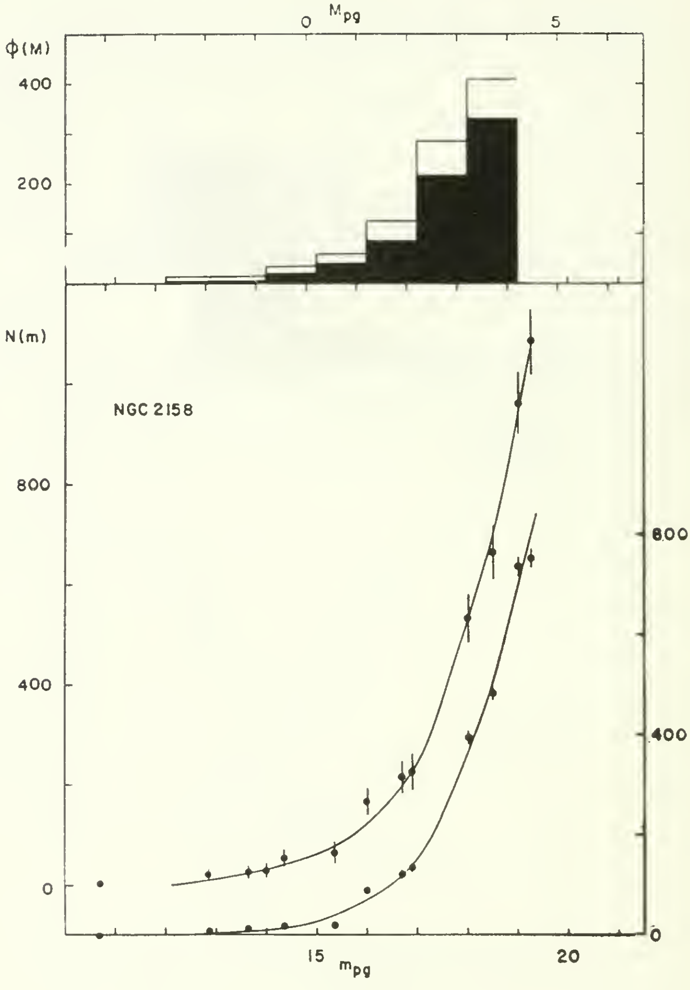

0
M_{pg}
5
$\Phi(M)$
400
200
N(m)
NGC 2158
800
400
0
800
400
0
15
m_{pg}
20

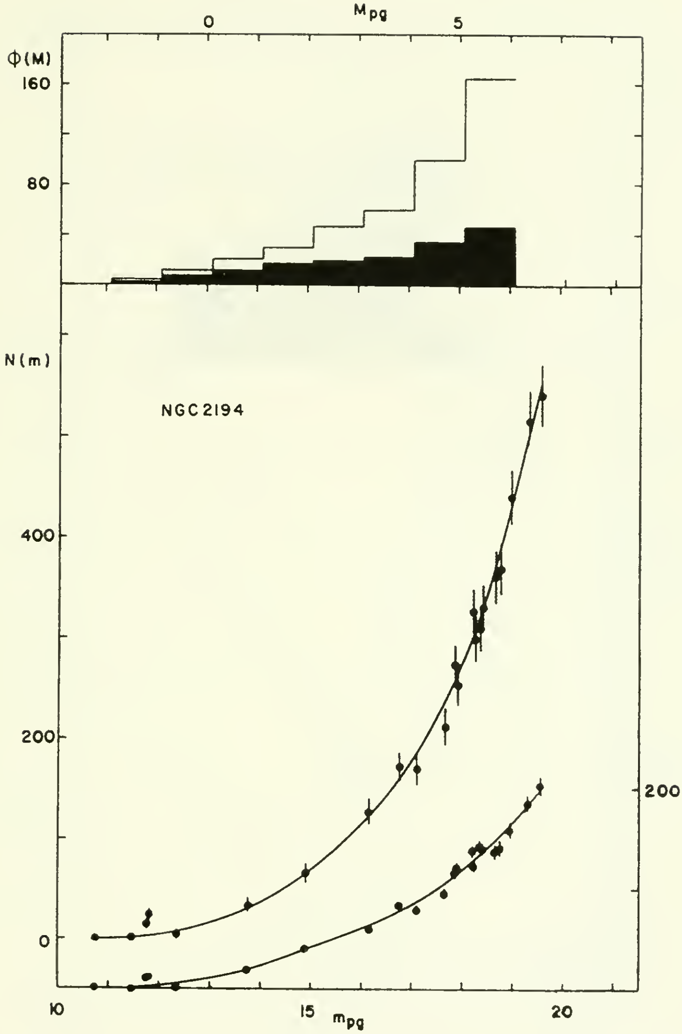

Mpg
0
5
Φ(M)
160
80
N(m)
NGC 2194
400
200
0
200
10
15
mpg
20

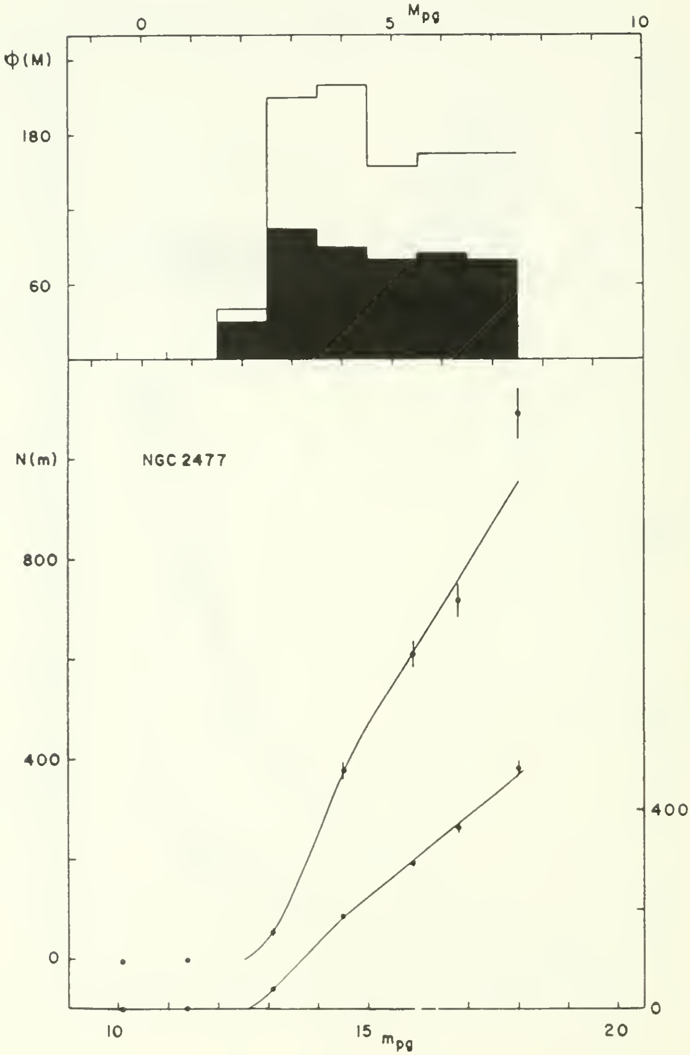
M_pg
0
5
10
Φ(M)
180
60
N(m)
NGC 2477
800
400
0
400
0
10
15
20
m_pg

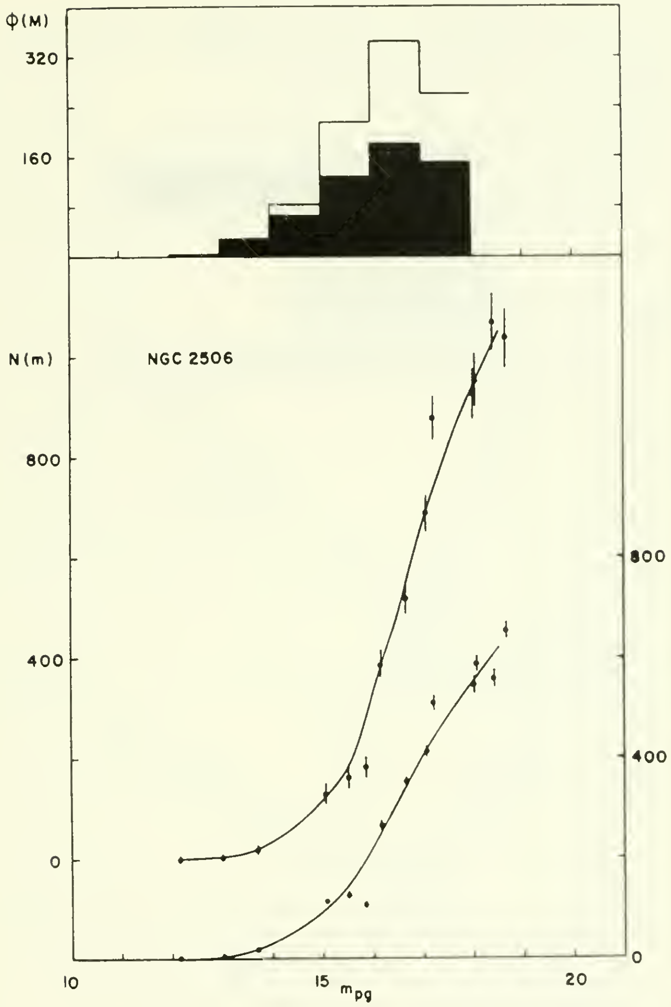
Φ(M)
320
160
N(m)
NGC 2506
800
400
0
800
400
0
10
15
m_{pg}
20

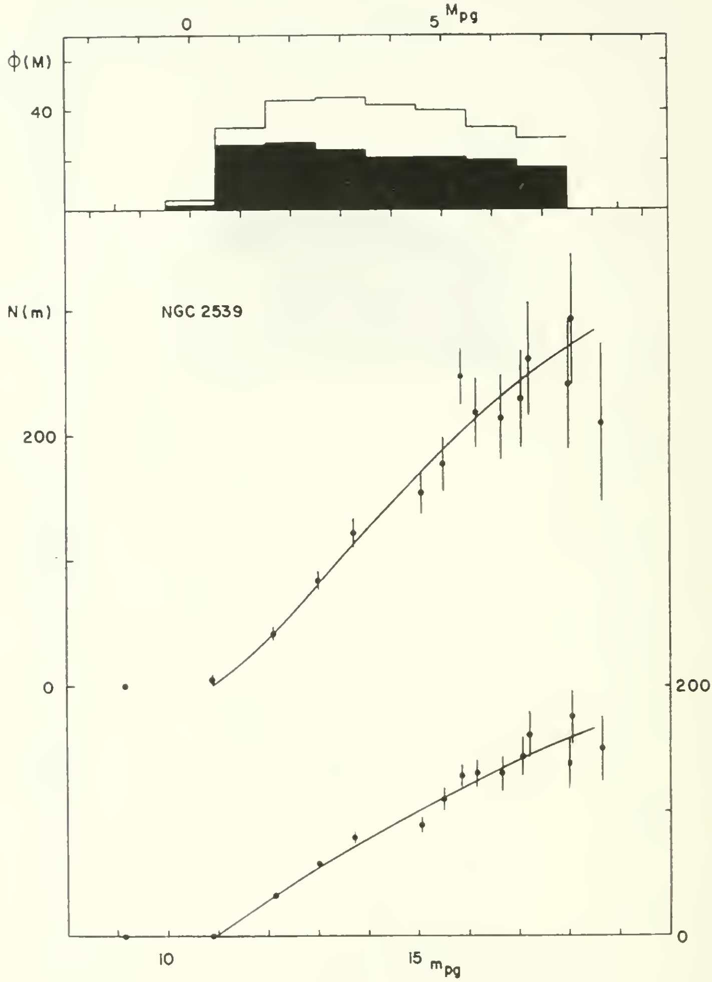
0
5 M_{pg}
ϕ(M)
40
N(m)
NGC 2539
200
0
200
0
10
15 m_{pg}

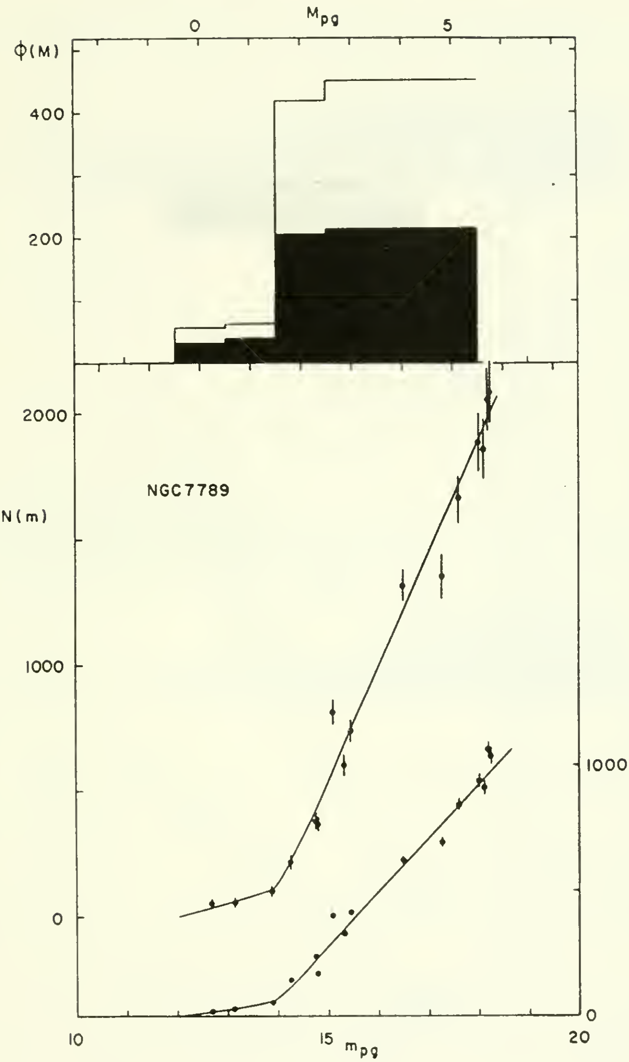

M_{pg}
0
5
$\phi(M)$
400
200
2000
NGC7789
N(m)
1000
0
1000
0
10
15
m_{pg}
20

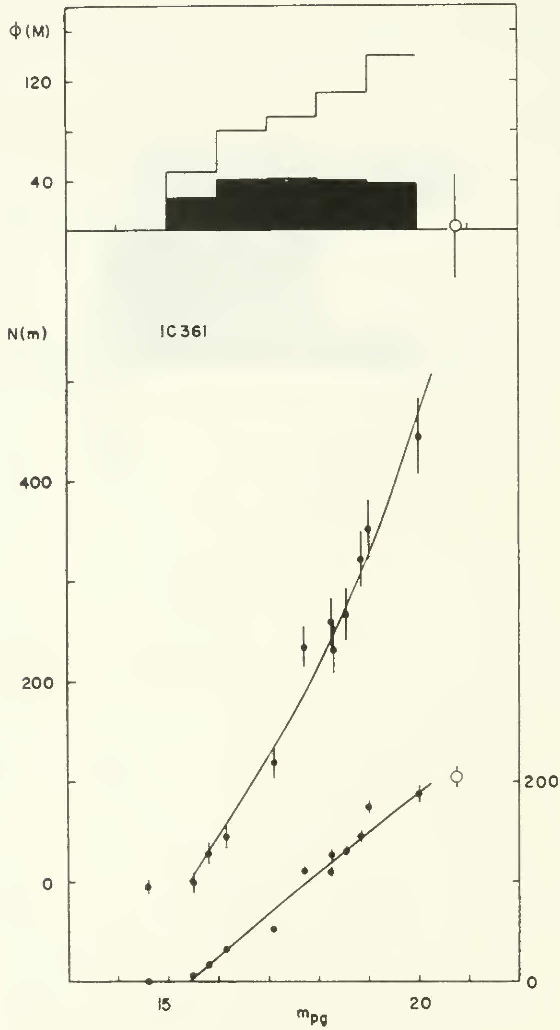

Φ(M)
120
40
N(m)
IC 361
400
200
0
200
0
15
20
m_{pg}

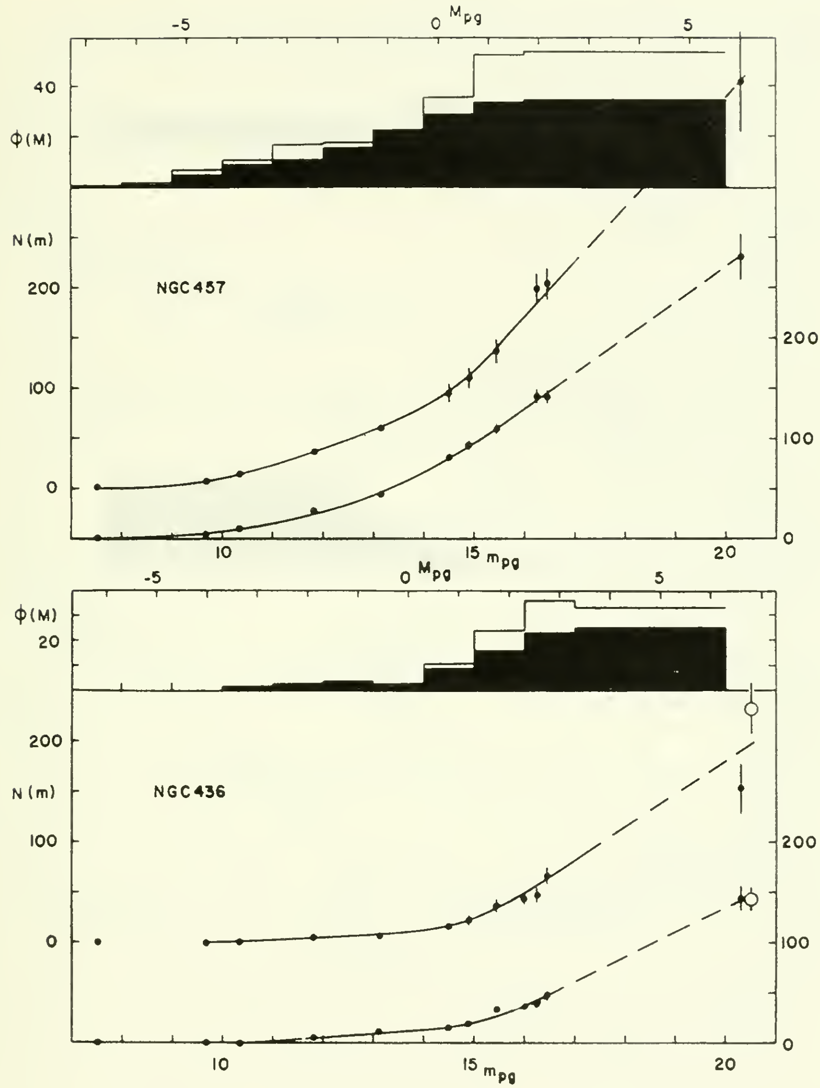
-5
0 M_{pg}
5
40
Φ(M)
N(m)
200
NGC457
100
0
200
100
0
10
15 m_{pg}
20
-5
0 M_{pg}
5
Φ(M)
20
200
N(m)
NGC436
100
0
200
100
0
10
15 m_{pg}
20

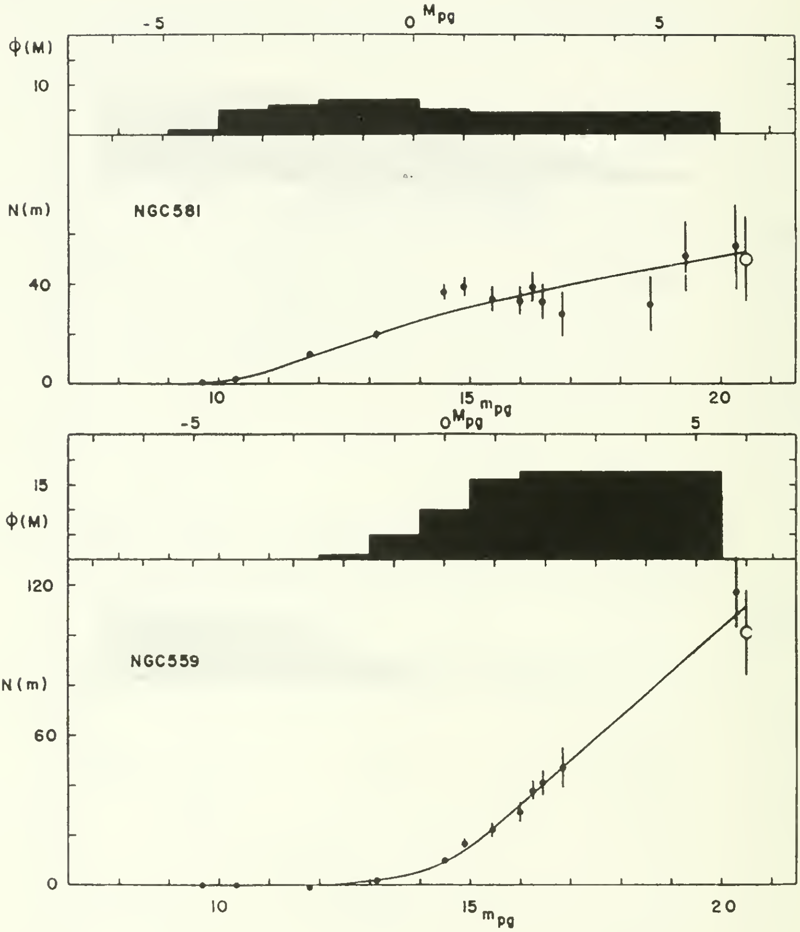

M_{pg}
-5
0
5
Φ(M)
10
N(m)
NGC581
40
0
10
15 m_{pg}
20
-5
0 M_{pg}
5
15
Φ(M)
120
NGC559
N(m)
60
0
10
15 m_{pg}
20

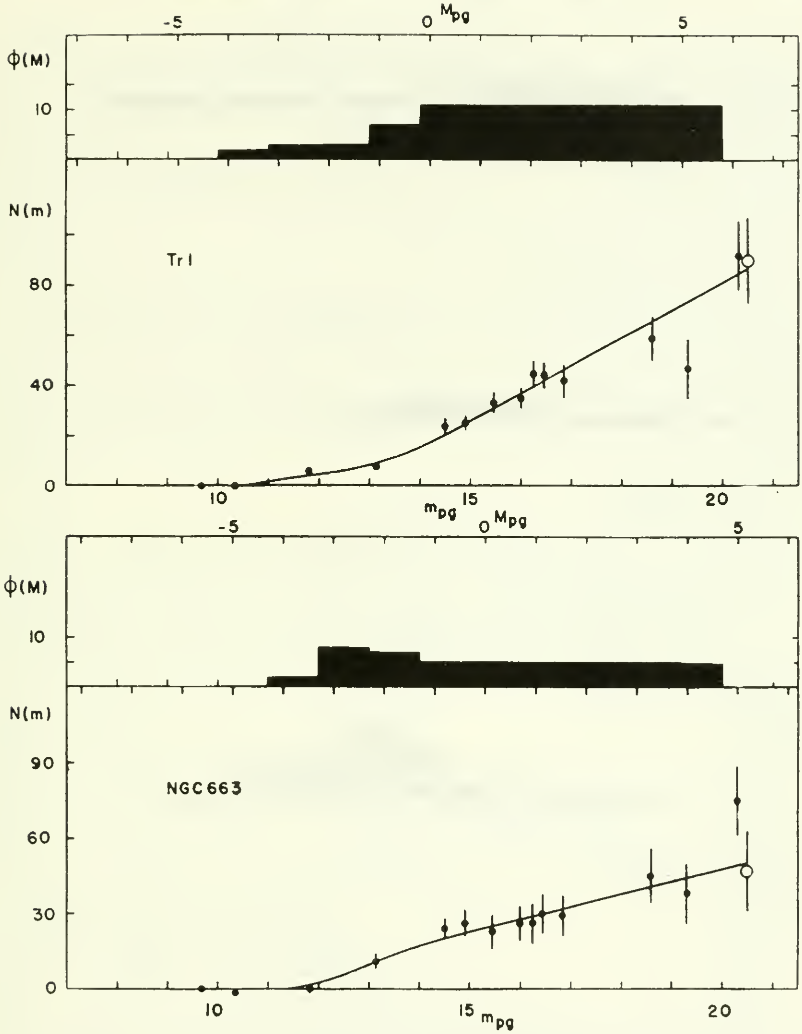
M_{pg}
-5
0
5
$\phi(M)$
10
N(m)
Tr I
80
40
0
10
15
20
m_{pg}
-5
0
M_{pg}
5
$\phi(M)$
10
N(m)
90
NGC663
60
30
0
10
15
m_{pg}
20

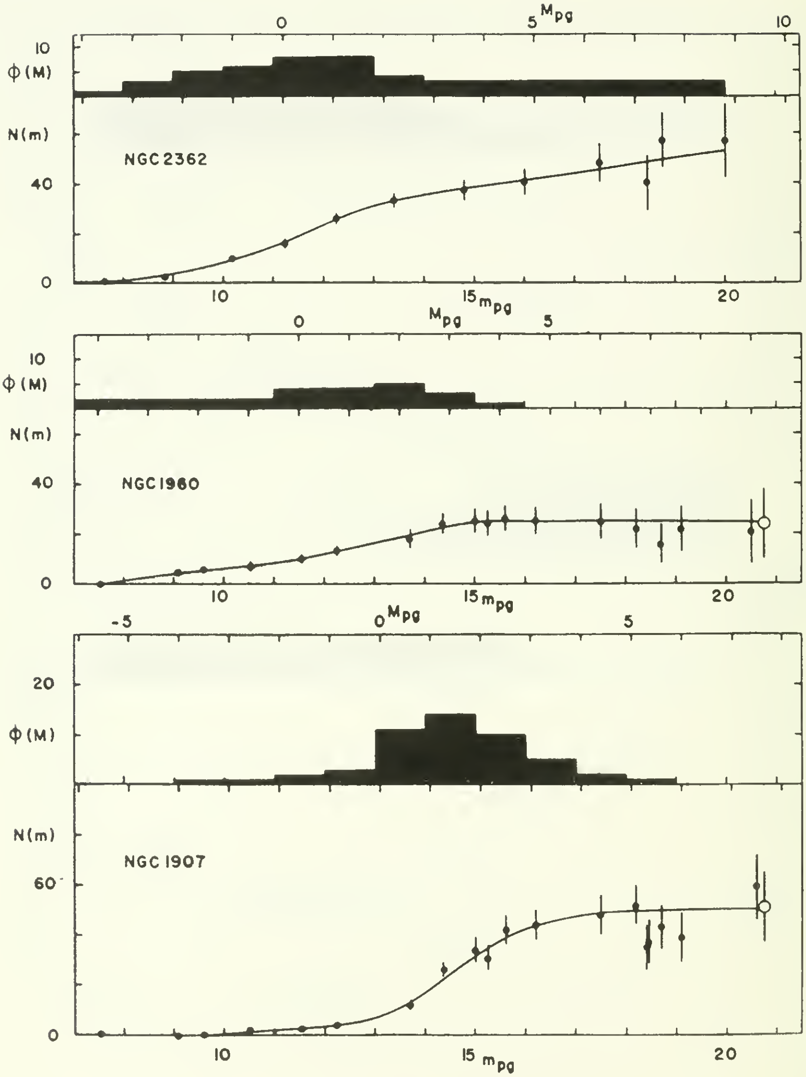

0
5 M pg
10
10
φ (M)
N(m)
NGC 2362
40
0
10
15 m pg
20
0
M pg
5
10
φ (M)
N(m)
NGC 1960
40
0
10
15 m pg
20
-5
0 M pg
5
20
φ (M)
N(m)
NGC 1907
60
0
10
15 m pg
20

Acknowledgements

The observations on which this investigation is based were obtained while one of us (S. v. d. B.) was a guest investigator at the Mount Wilson and Palomar Observatories on temporary leave from the Ohio State University. The hospitality which he enjoyed at Mount Wilson and at the California Institute of Technology is gratefully acknowledged. In particular it is a pleasure to thank Dr. I. S. Bowen for his kind co-operation and Dr. A. R. Sandage for a number of helpful discussions. The competent assistance of Mr. C. Kearns with the 48-inch telescope is also gratefully recorded.

We are also indebted to Dr. H. C. Arp for providing us with an unpublished photoelectric sequence in NGC 2158 in addition to a set of plates of the same cluster taken with the 200-inch telescope. Dr. A. R. Sandage kindly provided photoelectric sequences in NGC 188 and NGC 7789 and Dr. W. A. Baum gave us unpublished photoelectric sequences in a number of selected areas. Dr. M. S. Roberts gave us some of his unpublished data on luminosity functions of a few clusters.

Part of this investigation was supported by a grant from the Ontario Research Foundation.

References

Allen, C. W. 1955, "Astrophysical Quantities", (London: The Athlone Press) p. 180.
van den Bergh, S. 1957. *A. J.*, vol. 62, p. 100.
Bodén, E. 1951, *Uppsala Ann.*, vol. 2, no. 10.
Burbidge, E. M. and Sandage, A. R. 1958, *Ap. J.*, vol. 128, p. 174.
Chandrasekhar, S. 1942, "Principles of Stellar Dynamics", (Chicago: Univ. of Chicago Press) p. 234.
Cuffey, J. 1937a, *Harv. Ann.*, vol. 105, p. 403.
Cuffey, J. 1937b, *Harv. Ann.*, vol. 106, p. 39.
Cuffey, J. 1943, *Ap. J.*, vol. 97, p. 93.
Hiltner, W. A. 1956, *Ap. J. Suppl.*, vol. 2, p. 389.
Johnson, H. L. and Morgan, W. W. 1953, *Ap. J.*, vol. 117, p. 313.
Johnson, H. L. and Sandage, A. R. 1955, *Ap. J.*, vol. 121, p. 616.
Johnson, H. L. 1957, *Ap. J.*, vol. 126, p. 121.
Johnson, H. L. 1959, *Lowell Obs. Bull.*, vol. 4, p. 37.
King, I. R. 1959, *A. J.*, vol. 64, p. 351.
Kruspán, E. 1959, *Zs. f. Ap.*, vol. 48, p. 1.
Lindblad, P. O. 1954, *Stockholm Ann.*, vol. 18, no. 1.
Pesch, P. 1959, *Ap. J.*, vol. 130, p. 764.
Sandage, A. R. 1957, *Ap. J.*, vol. 125, p. 422.
Sawyer, H. B. 1930, *Harvard Obs. Bull.*, no. 875, p. 16.
Schmidt, M. 1959, *Ap. J.*, vol. 129, p. 243.
Walker, M. F. 1956, *Ap. J. Suppl.*, vol. 2, p. 365.
Zug, R. S. 1933, *Lick Obs. Bull.*, vol. 16, p. 119.